

# Tsunami potential of major restraining bends along submarine strike-slip faults

Mark R. Legg<sup>1</sup> and Jose C. Borrero<sup>2</sup>

<sup>1</sup>*Legg Geophysical, Huntington Beach, California, U.S.A.*

<sup>2</sup>*Department of Civil Engineering, University of Southern California, Los Angeles, California, U.S.A.*

**Abstract.** Strike-slip faults, with mostly horizontal displacements, are rarely considered capable sources of destructive tsunamis. Real strike-slip faults are sinuous, however, with curved and offset traces where local areas of uplift or subsidence occur. At fault bends or offsets where the lateral slip is restrained, seafloor uplift during large submarine earthquakes may generate locally destructive tsunamis. To investigate tsunami potential along the San Diego, California coast, we model uplift along a major restraining bend of the offshore San Clemente fault zone. The 60 km long, 15° oblique fault segment has created an 875 km<sup>2</sup> area of seafloor uplift. Maximum uplift based on seafloor relief is 430 m, although the total tectonic uplift shown in seismic profiles is about 720 m. To calibrate elastic dislocation models for earthquake source deformation, seafloor morphology and relative uplift from detailed Sea Beam bathymetry are scaled for a single-event fault displacement. Hydrodynamic models developed at USC are then applied to propagate the tsunami to the adjacent coastline to estimate wave run-up. We find that elastic dislocation models used to estimate tsunami potential underestimate the seafloor displacement (<1 m). Meters of fault slip were observed during recent large earthquakes ( $M \geq 7$ ) and on seafloor fault scarps viewed from submersible on the San Clemente fault. Many large restraining bends exist on several offshore fault zones, thereby posing a greater local tsunami risk for the southern California coast than previously stated.

## 1. Introduction

Strike-slip faulting, with predominately horizontal fault offsets, is often ignored with regard to tsunami potential. Tsunamis generated by tectonic displacements usually occur in areas of dip-slip faulting, such as the major thrust faults along subduction zones or normal faulting in extensional regimes. Recent tsunamis associated with major strike-slip earthquakes, such as the 1994 Mindoro, Philippines earthquake (Daag *et al.*, 1995), showed that strike-slip faulting has destructive tsunami potential. In most cases, however, the tsunamis occurring after major strike-slip earthquakes were considered due to submarine landslide, not to direct tectonic deformation of the seafloor.

Crustal-scale strike-slip faults do not have simple straight traces involving only horizontal displacement. Instead, their traces are irregular and fault complexity usually creates major regions of fault normal displacements and vertical offsets. In particular, where the fault curves or steps so as to obstruct the simple horizontal slip, a restraining bend or fault stepover occurs and the region along the fault is uplifted (Fig. 1; Crowell, 1974; McClay and Bonora, 2001). Likewise, where the fault curves or steps in the opposite

---

<sup>1</sup>Legg Geophysical, 16541 Gothard Street, Suite #107, Huntington Beach, CA 92647, U.S.A. (mrlegg@attglobal.net)

<sup>2</sup>University of Southern California, Department of Civil Engineering, KAP 210, Los Angeles, CA 90089-2351, U.S.A. (jborrero@usc.edu)

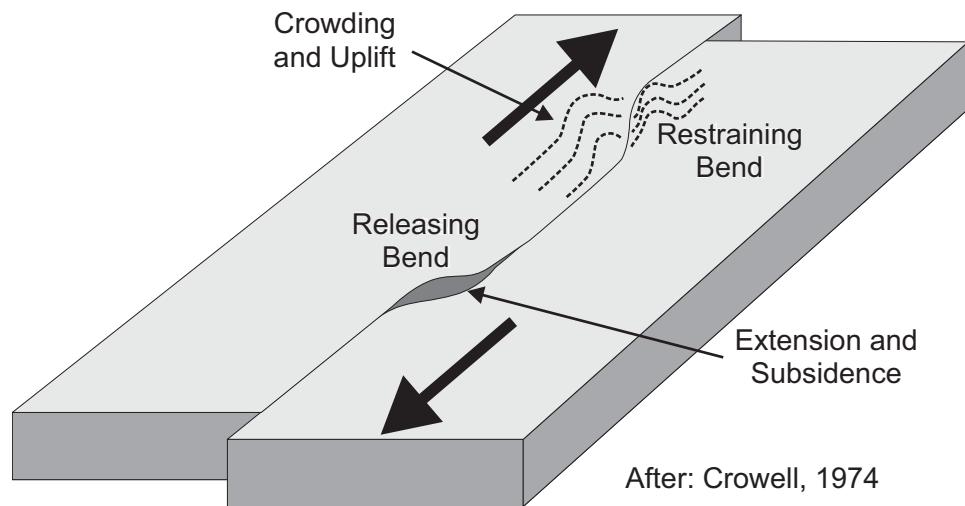


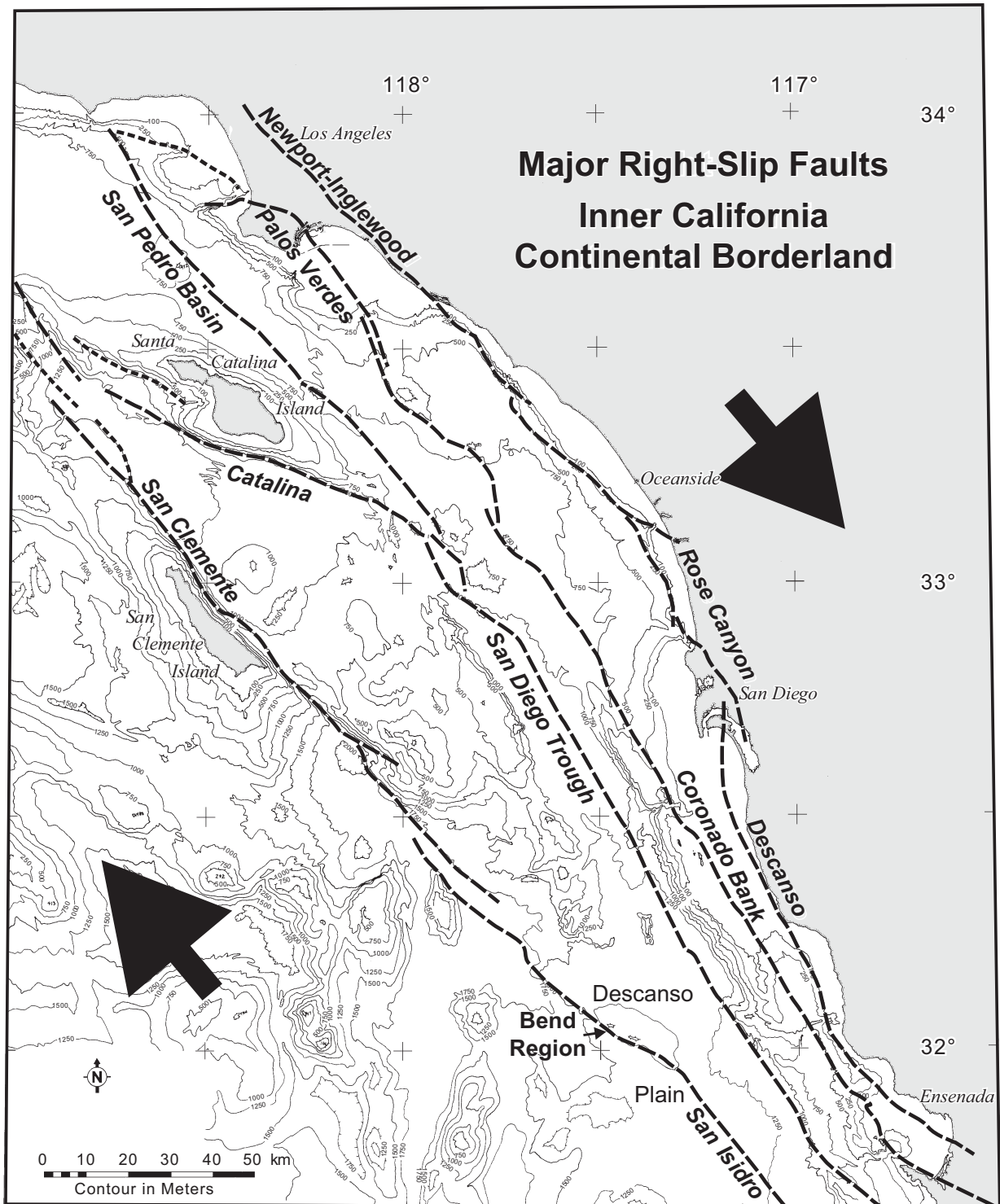
**Figure 1:** Sketch showing areas of convergence at restraining bends and areas of extension at releasing bends along sinuous strike-slip faults.

manner, to create a zone of extension, a releasing bend or pull-apart occurs and the region along the fault subsides (Fig. 1; Crowell, 1974; McClay and Dooley, 1995).

Along major strike-slip fault zones, such as comprise the Pacific-North America (PAC-NOAM) transform plate boundary, restraining and releasing fault segments are interspersed along the fault traces. In southern California, where the plate boundary is more than 200 km wide, the numerous ridges and basins of the offshore California Continental Borderland directly result from oblique fault movements along these sinuous faults (Fig. 2; Shepard and Emery, 1941; Vedder, 1987; Legg, 1985; Legg and Kennedy, 1991). Meters of vertical seafloor movement in these areas of oblique-faulting, during large strike-slip earthquakes ( $M \geq 7$ ), are likely to generate destructive local tsunamis. To evaluate local tsunami potential for southern California, we model the seismogenic fault uplift, tsunami generation, and potential wave run-up for a major restraining bend along the submarine San Clemente fault zone (Fig. 3).

## 2. Tsunami Potential of a Major Restraining Bend Along the San Clemente Fault Zone

The San Clemente fault zone is the longest (>400 km) and most active fault zone of the southern California offshore region (Legg, 1985; Legg *et al.*, 1989). Morphology of the seafloor along the fault (Legg *et al.*, 1989) and earthquake focal mechanisms (Legg, 1980) show that the San Clemente fault is predominately of right-slip character. Yet, across the Borderland, oblique fault movements have produced major seafloor escarpments, exceeding 1000 m in height, that bound large crustal blocks, exceeding 100–1000 km<sup>2</sup> in area



After Legg, 1985; Vedder, 1987; Fischer and Mills, 1991; Legg and Kennedy, 1991

**Figure 2:** Map showing the major active strike-slip faults of the Inner California Continental Borderland, which tend to have sinuous traces with many restraining and releasing bends. This study focuses on the bend region of the San Clemente–San Isidro fault zone.

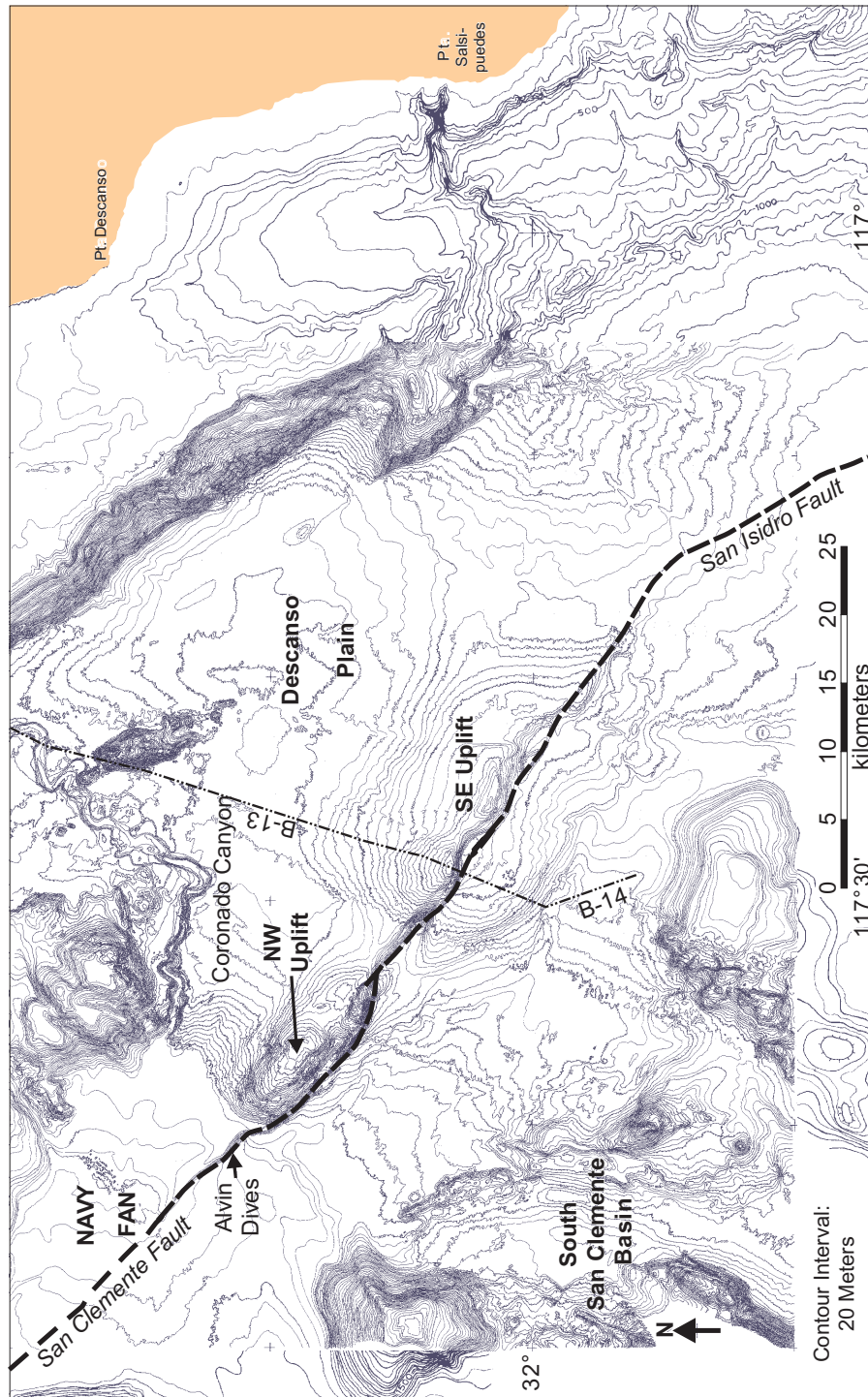


**Figure 3:** Map showing seafloor contours in the bend region of the San Clemente fault zone based upon SeaBeam swath mapping and older echo soundings (after Legg *et al.*, 1999). The tsunami modeling for this study focuses on the larger, southeast uplift region for simplicity. Location of seismic profile B-13/14 (Fig. 4) is also shown.

(Fig. 2). Although many of these crustal blocks originally formed during earlier oblique-extensional (transtensional) tectonic episodes along the evolving PAC-NOAM transform boundary, oblique fault movement during late Quaternary time (past 700,000 yrs) continues on the San Clemente fault system (Legg and Kennedy, 1991).

Within the Descanso Plain (Figs. 2 and 3), a broad seafloor basin offshore northern Baja California, Mexico, the San Clemente fault curves through a major restraining bend. Here, a 60 km long fault segment turns about 15° oblique to the average fault strike and the PAC-NOAM transform relative motion vector. Because the fault turns more to the west, a left bend along strike, the general northwest movement of the Pacific plate is impeded, causing seafloor uplift (Fig. 3). Former horizontal layered sediments (turbidites) deposited from nearby submarine fans fill the Descanso Plain and show the tectonic uplift in seismic reflection profiles across the region (Fig. 4; Legg, 1985; Legg and Kennedy, 1991). The shape of the seafloor uplift, and structural contours of buried turbidite horizons, directly measure the displacement field associated with the fault convergence and oblique movement (transpression). By assuming that the shape and relative uplift of seafloor resulted from accumulated tectonic deformation during large earthquakes, we can model the seafloor uplift for realistic single earthquake events and estimate the resulting tsunami run-up.

Recent observations from the DSV *Alvin* (submersible) near Navy Fan (Fig. 3) find several seafloor fault scarps that represent actual seafloor uplift during the most recent earthquakes on this section of the San Clemente fault (Goldfinger *et al.*, 2000). The largest scarps are 1–3 m in overall height, and lineaments along the largest and most recent scarp suggest oblique movement, about 15 degrees from horizontal. Fault displacements of 1–3 m are generally associated with large earthquakes ( $M > 6.5$ ), and if substantial areas of seafloor are uplifted, a local tsunami may result. A recent example was the 1989 Loma Prieta earthquake ( $M = 7.1$ ) along the San Andreas fault zone where blind faulting below 5 km subsurface depth suffered vertical slip of about 1.3 m and horizontal right-slip of about 1.9 m (Plafker and Galloway, 1989). Even though the 1989 faulting was onshore, in the Santa Cruz Mountains, the broad zone of uplift associated with the earthquake reached the Pacific Coast and produced a small tsunami (Schwing *et al.*, 1990; McCarthy *et al.*, 1993).

In detail, faulting along the bend region of the San Clemente fault zone shows some complexity (Fig. 3), with two prominent areas of seafloor uplift along the transpressional segment. The southeast uplift is larger, about 30 km long by 20 km wide, and asymmetric in cross-section with the northeast block higher (Fig. 4). The northwest uplift is only about 16 km long, narrower at 9 km wide, and more symmetrical with steep southwest and northeast flanks. Total seafloor relief for both uplift areas is similar, about 680–700 m, separated by a 4 km long saddle with relief of about 340 m. A third shorter, 9-km length, lower relief, 80–90 m, and asymmetrical uplift exists along the northwest end of the bend region at Navy Fan. The principal displacement zone of recent faulting lies along the southwest flank of the major uplift throughout the bend region, implying that the fault dips

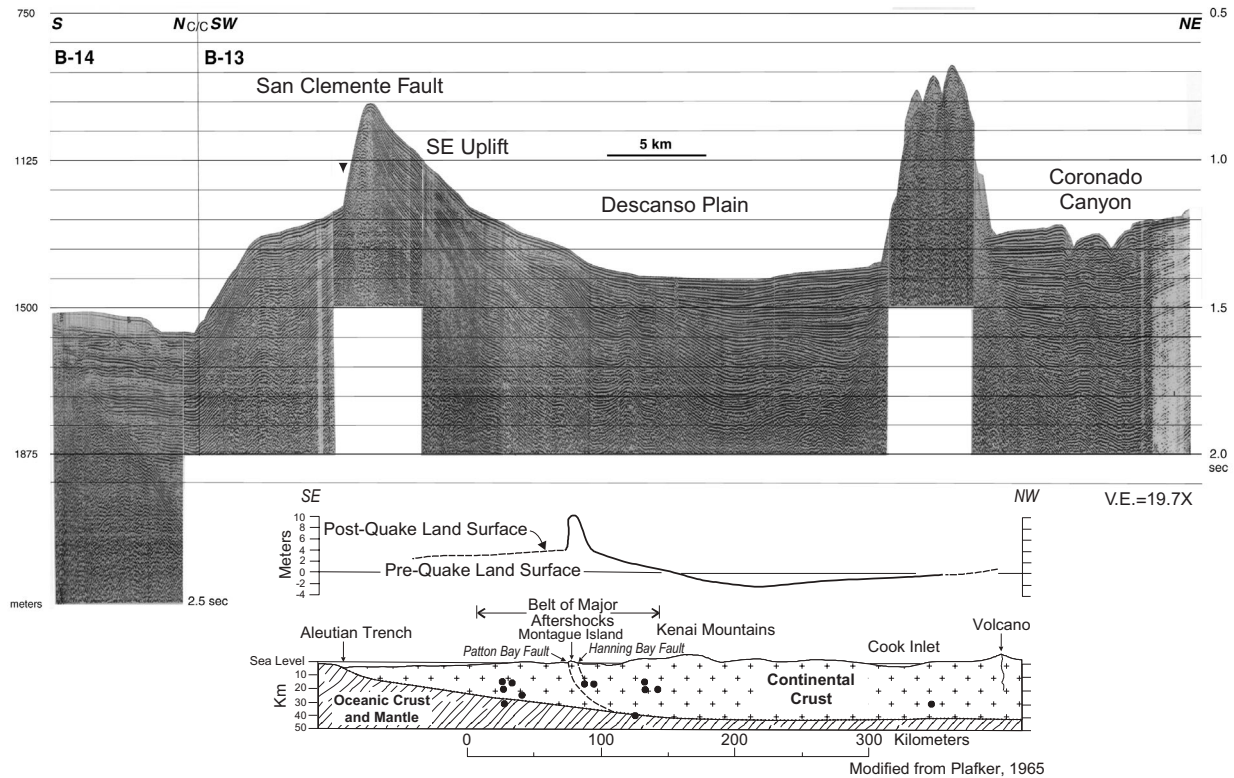


**Figure 4:** Single channel sparker seismic reflection profile across the major seafloor uplift in the bend region of the San Clemente fault zone. The seafloor is relatively uplifted on both sides of the fault trace, with greater uplift to the northeast. Inset at bottom shows measured uplift for profile across Montague Island following the 1964 Great Alaska earthquake ( $M = 9.2$ ; after Plafker, 1965) with geological interpretation showing shallow high-angle faulting above the major low-angle subduction thrust. In profile, the pattern of uplift from the 1964 earthquake resembles that observed on the seafloor modeled in this study.

to the northeast in this area. Notwithstanding the sinuous, en echelon, and anastomosing character of individual scarps along the principal displacement zone, the overall trace of the active faulting is remarkably straight, with a  $305^\circ$  strike, consistent with a high-angle strike-slip fault.

## 2.1 Fault model for tsunami generation

For this preliminary analysis, designed to estimate tsunami characteristics, only the southeast uplift is modeled. The simple model provides a broad uplift pattern that should match the seafloor morphology in a gross sense. For the long wavelengths of concern for tsunami generation, the more complex details in the fault trace and uplift shape can be ignored. By ignoring the second large uplift to the northwest, however, the estimates of tsunami magnitude may understate the maximum expected tsunami amplitude. Nevertheless, a realistic estimate of tsunami magnitude generated by major restraining bends along submarine strike-slip faults is obtained.

In the bend region, both sides of the fault are uplifted above the sur-

**Table 1:** Fault parameters for seafloor uplift and tsunami generation.

Fault	Length (km)	Width (km)	Strike (degrees)	Dip (degrees)	Slip-rake (degrees)	Slip-amount (m)	Focal depth (km)
Shallow (surface)	30	8	305	70 NE	162	8	7.6
Deep (blind)	25	14	270	48 N	134	8	16

rounding basin, with greater uplift on the northeast side. Elastic dislocation models used to predict finite deformations from dip-slip earthquakes typically show one side of the fault moving up and the other side down relative to an original horizontal surface. Consequently, a single, northeast-dipping, planar fault model will not accurately model the seafloor uplift in the bend region. Tectonic uplift measured after the 1964 Alaska earthquake ( $M = 9.2$ ) showed a similar pattern of asymmetrical uplift in the vicinity of Montague Island (Fig. 4 inset), with an overall uplift on both sides of the Patton Bay fault scarp (Plafker, 1965). A geologic model with a shallow high-angle fault (the Patton Bay fault) above a deeper, low-angle, subduction thrust fault was inferred to explain the observed pattern of uplift. In this study, we use a similar two-fault model, with a shallow, high-angle ( $70^\circ$  NE dip) fault above a deeper, low-angle ( $25\text{--}48^\circ$  N dip) fault (Table 1). Both faults are right-lateral, oblique reverse-slip in character, with the slip vector set to allow rigid movement of the hanging wall block constrained by the fault geometry. The strike ( $305^\circ$ ) of the shallow fault was set to the measured strike of the principal displacement zone as mapped from the high-resolution swath bathymetry (Fig. 3). The shallow fault dip was set at  $70^\circ$ , similar to that observed for the 1989 Loma Prieta earthquake (Plafker and Galloway, 1989). Also, the overall shape of the displacement pattern predicted for a single fault, with  $70^\circ$  dip, compares well to the seafloor morphology. The strike of the deeper, low-angle, oblique-thrust fault was set at  $270^\circ$  (east–west) because the boundaries of the seafloor uplift appear to have a north–south trend, consistent with a north-dipping, west-trending, blind fault. This north trend is most apparent along the eastern edge of the uplift (Fig. 3), although in part, this character may result from north-trending normal faults and grabens along the eastern half of the uplift. The model with the steeper,  $48^\circ$ N dip, blind fault at depth provided a better fit to the observed seafloor morphology with an elongated, northwest-trending, uplift pattern. A second model with a low-angle,  $25^\circ$ N dip, blind fault produced a seafloor uplift that was more rectangular in shape, with subsidence to the northwest, unlike the observed seafloor morphology.

A problem encountered in the elastic dislocation model is that the predicted seafloor uplift is much smaller than the fault slip at the hypocenter (focal depth). For example, a maximum slip of 4 m on the fault at the focal depth of 7.6 km yields a predicted seafloor uplift of only about 1 m. Such a result may be valid for blind faulting, as in the 1989 Loma Prieta oblique-reverse earthquake, where surface uplift was significantly smaller ( $\sim 0.5$  m) than the inferred maximum fault slip at depth (1–2 m, Plafker and Galloway,

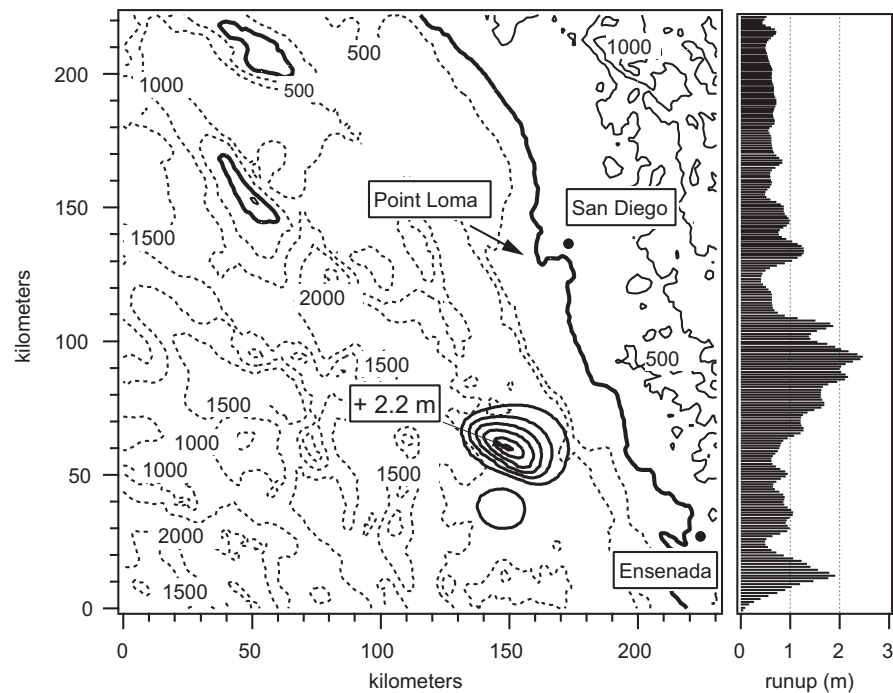


**Figure 5:** Location map and run-up plot. The thick black lines are the seismic deformations associated with the earthquake. The run-up along the coast is plotted on the right.

1989). Yet, for large strike-slip earthquakes with surface fault rupture, maximum surface fault slip is comparable to calculated subsurface slip (e.g., 2–6 m, 1992 Landers, Wald and Heaton, 1994), and local areas of slightly smaller vertical slip ( $\sim 2$  m) are present. Inferred single-event fault scarps on the submarine San Clemente fault in the bend region are 1–3 m high, comparable to scarps observed in recent earthquakes with subaerial surface fault rupture. Therefore, we scaled the hypocentral slip maximum upward, to 8 m, in order to produce a seafloor uplift of about 2 m. This may still underestimate the seafloor displacement from real earthquakes on the San Clemente fault zone, especially if the horizontal slip exceeds the vertical slip by a large factor ( $>2$ ) or a longer fault rupture occurs ( $>30$ – $40$  km).

## 2.2 Tsunami modeling

The tsunami modeling process can be broken into three parts, generation, propagation, and run-up (Liu *et al.*, 1991; Titov and González, 1997). The generation phase includes the formation of an initial disturbance on the ocean surface due to a coseismic deformation of the sea floor. In this case, the initial condition for the long wave propagation is obtained directly from the expected coseismic deformation of the earth's surface. The deformation on the sea floor is modeled using Okada's (1985) formulas for surface deformation due to shear and tensile faults in a homogeneous, elastic, half space.

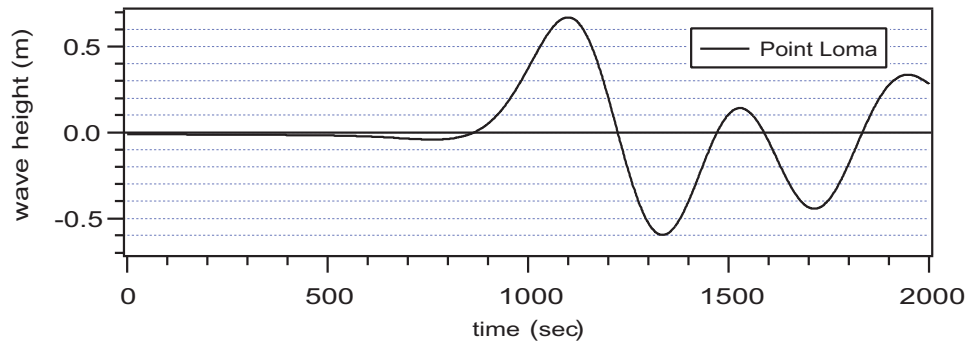


**Figure 6:** Synthetic wave gauge record off of Point Loma, near the entrance to San Diego Bay. A water surface fluctuation of over 1 m is modeled.

The deformation field modeled by these equations is translated directly to the water surface and used as an initial condition for the propagation and run-up phases.

For tsunami propagation and run-up, the model known by the acronym MOST (Titov and González, 1997) was employed. This model uses the fully non-linear, depth averaged, shallow water wave equations in characteristic form to simulate the propagation of long waves over an arbitrary bathymetry. For run-up it uses a moving boundary algorithm (Titov and Synolakis, 1995; Titov and González, 1997).

For this initial study, a 1-min bathymetry and topography grid was used over the simulation area. The initial condition was located according to geophysical data, i.e., the SeaBeam bathymetry and fault mapping. The initial surface displacement was modeled using the seismic parameters for a compound fault model shown in Table 1.

Figure 5 shows the location of the initial surface displacement and the computed run-up along the right-hand shoreline. Values are highest along the Mexican coast between San Diego and Ensenada with run-up heights reaching 2.5 m. There are concentrations of higher run-up at Point Loma, near San Diego, and at Punta Banda near Ensenada in Baja California, Mexico. A virtual wave gauge record from a gauge located along the 20 m isobath just off of Point Loma is shown in Fig. 6. The wave gauge record shows a water surface fluctuation of over 1 m that begins as a leading elevation wave approximately 900 s after the wave was generated. The initial water motion takes approximately 600 s to complete. Such a long period oscillation has the potential to generate substantial currents in the narrow openings of harbors—a phenomenon observed in other tsunamis (Borrero *et al.*, 1995). It should be noted that the entrance to San Diego Bay faces directly into the oncoming wave and would be particularly vulnerable to a tsunami generated in this region. However, much more detailed studies would be needed to accurately assess the impact of this tsunami source on San Diego Bay and the marine facilities it contains.

### 3. Summary and Conclusions

Tsunami run-up amplitudes of a few meters are predicted along the southern California, U.S.A., and northern Baja California, Mexico, coast due to large earthquakes ( $M > 7$ ) along the bend region of the offshore San Clemente fault zone. Tsunamis of similar size generated in recent earthquakes along active subduction zones have been locally destructive, e.g., Sulawesi Island (Pelinovsky *et al.*, 1997). With a travel time to the coast of less than 20 min, no official warning would reach affected populations before the first wave maximum reaches the nearby coast. Because only a part of the overall uplift in the bend region was modeled, larger fault ruptures and seafloor deformations may occur with the potential for larger tsunami run-up along the adjacent coast. Further amplification at narrow canyons along steep coastal bluffs could also result in somewhat higher local inundation. Frequency or probability of occurrence for local tsunamis generated by the major fault zones offshore southern California remains to be determined, but may be less than 1,000 years recurrence interval. Seafloor scarps observed from the Alvin submersible, 1–3 m in height, suggest that several events have occurred along the San Clemente fault in recent prehistory.

This study is part of an ongoing research initiative to reassess the tsunami hazard in California and along the U.S. West Coast. The results of this simulation are being integrated with other scenarios to generate a series of comprehensive tsunami inundation maps for the state of California.

**Acknowledgments.** The authors wish to acknowledge the assistance of the Southern California Earthquake Center in obtaining the SeaBeam data, and Peter Lonsdale and other chief scientists who shared these data with us. Dr. Legg's research was supported by the U.S. Geological Survey (USGS), Department of the Interior, under USGS award number 01HQGR0017. The views and conclusions contained in the document are those of the authors and should not be interpreted as necessarily representing the official policies, either expressed or implied, of the U.S. Government.

### 4. References

- Borrero, J., M. Ortiz, V. Titov, and C. Synolakis (1995): Field survey of Mexican tsunami produces new data, unusual photos. *Eos Trans. AGU*, 88, 85, 87–88.
- Crowell, J.C. (1974): Origin of late Cenozoic basins in southern California. In *Tectonics and Sedimentation*, edited by W.R. Dickinson, Society of Economic Paleontologists and Mineralogists, Tulsa, Special Publication 22, 190–204.
- Daag, A.S., P.J. de los Reyes, B.S. Tubianosa, D.V. Javier, and R.S. Punongbayan (1995): Tsunami deposit of the 15 November 1994 Mindoro earthquake, Philippines. *Proceedings, Tsunami Deposits, Geologic Warnings of Future Inundation*, University of Washington, Seattle, 22–23 May, 1995, 3.
- Goldfinger, C., M. Legg, and M. Torres (2000): New mapping and submersible observations of recent activity on the San Clemente fault. *Eos Trans. AGU*, 81, 1069.
- Legg, M.R. (1980): Seismicity and tectonics of the inner continental borderland of southern California and northern Baja California, Mexico. M.S. thesis, University of California, Santa Diego, 60 p.

- Legg, M.R. (1985): Geologic structure and tectonics of the inner continental borderland offshore northern Baja California, Mexico. Ph.D. dissertation, University of California, Santa Barbara, 410 pp.
- Legg, M.R., B.P. Luyendyk, J. Mammerickx, C. de Moustier, and R.C. Tyce (1989): SeaBeam survey of an active strike-slip fault—The San Clemente fault in the California Continental Borderland. *J. Geophys. Res.*, *94*, 1727–1744.
- Legg, M.R., and M.P. Kennedy (1991): Oblique divergence and convergence in the California Continental Borderland. In *Environmental Perils of the San Diego Region*, edited by P.L. Abbott and W.J. Elliott, San Diego Association of Geologists Guidebook, 1–16.
- Legg, M.R., D.E. Einstein, and H.D. Wang (1999): Deformation history of a major restraining bend along a right-slip fault: The San Clemente fault offshore northern Baja California, Mexico. *Proceedings and Abstracts, 1999 Annual Meeting, Southern California Earthquake Center*, Palm Springs, CA, 26–29 September 1999, 74–75.
- Liu, P.L.-F., C.E. Synolakis, and H. Yeh (1991): Impressions from the First International Workshop on Long Wave Run-up. *J. Fluid Mech.*, *229*, 675–688.
- McCarthy, R.J., E.N. Bernard, and M.R. Legg (1993): The Cape Mendocino earthquake: A local tsunami wakeup call? *Proceedings of the Eighth Symposium on Coastal and Ocean Management*, New Orleans, Louisiana, 19–23 July 1993, 2812–2828.
- McClay, K., and T. Dooley (1995): Analog models of pull-aparts. *Geology*, *23*, 711–714.
- McClay, K., and M. Bonora (2001): Analog models of restraining stepovers in strike-slip fault systems. *AAPG Bull.*, *85*, 233–260.
- Okada, Y. (1985): Surface deformation due to shear and tensile faults in a half-space. *Bull. Seismol. Soc. Am.*, *75*, 1135–1154.
- Pelinovsky, E., D. Yuliadi, G. Prasetya, and R. Hidayat (1997): The January 1, 1996 Sulawesi Island tsunami. *Science of Tsunamis, Int. J. Tsunami Soc.*, *15*, 107–123.
- Plafker, G. (1965): Tectonic deformation associated with the 1964 Alaska earthquake. *Science*, *148*, 1675–1687.
- Plafker, G., and J.P. Galloway (1989): Lessons Learned from the Loma Prieta, California, Earthquake of October 17, 1989. *U.S. Geological Survey Circular 1045*, 48 p.
- Schwing, F.B., J.G. Norton, and C.H. Pilskaln (1990): Earthquake and bay—Response of Monterey Bay to Loma Prieta earthquake. *Eos Trans. AGU*, *71*, 250–252.
- Shepard, F.P., and K.O. Emery (1941): Submarine topography off the southern California coast—Canyons and tectonic interpretation. *Geological Society of America Special Paper 31*, 171 p.
- Titov, V., and C. Synolakis (1995): Modeling of breaking and non-breaking long-wave evolution and runup using VTCS-2. *J. Waterway Port Coast. Ocean Eng.*, *121*(6), 308–316.
- Titov, V., and F. González (1997): Implementation and testing of the method of splitting tsunami (MOST) model. *NOAA Technical Memorandum ERL PMEL-112*, Pacific Marine Environmental Laboratory, Seattle, WA, 11 pp.
- Vedder, J.G. (1987): Regional geology and petroleum potential of the southern California borderland. In *Geology and Resource Potential of the Continental Margin of Western North America and Adjacent Ocean Basins, Beaufort Sea to Baja California*, edited by D.W. Scholl, A. Grantz, and J.G. Vedder, Circum-Pacific Council for Energy and Mineral Resources, Houston, Texas, *Earth Science Series*, *6*, 403–447.

Wald, D.J., and T.H. Heaton (1994): Spatial and temporal distribution of slip for the 1992 Landers, California, earthquake. *Bull. Seismol. Soc. Am.*, 84, 668–691.